

Magnetic properties of $(\text{VO})_2\text{P}_2\text{O}_7$ from frustrated interchain coupling

G. S. Uhrig

Institut für Theoretische Physik, Universität zu Köln, D-50937 Köln, Germany

B. Normand

Institut für Physik, Universität Basel, Klingelbergstrasse 82, CH-4056 Basel, Switzerland

(Received 28 July 1998)

Neutron-scattering experiments on $(\text{VO})_2\text{P}_2\text{O}_7$ reveal both a gapped magnon dispersion and an unexpected, low-lying second mode. The proximity and intensity of these modes suggest a frustrated coupling between the alternating spin chains. We deduce the minimal model containing such a frustration, and show that it gives an excellent account of the magnon dispersion, static susceptibility, and electron-spin resonance absorption. We consider two-magnon states which bind due to frustration, and demonstrate that these may provide a consistent explanation for the second mode. [S0163-1829(98)50646-7]

Vanadyl pyrophosphate [$(\text{VO})_2\text{P}_2\text{O}_7$, abbreviated VOPO]¹ is a low-dimensional quantum magnetic system composed of $S = \frac{1}{2}$ V^{4+} ions. These have Heisenberg antiferromagnetic (AF) interactions, and a singlet ground state¹ with spin gap $\Delta = 3.1$ MeV. Based on susceptibility and neutron-scattering experiments on powders, VOPO has been compared in detail to spin-ladder and alternating-chain models,² both of which were found to be consistent with the data. Rising interest in spin ladders, along with the assumption that the strongest exchange paths would be those between V^{4+} ions with the smallest separations, led to a preference^{1,2} for the ladder conformation, and for several years VOPO was quoted as the first known spin ladder system.

This picture was conclusively debunked by Garrett and co-workers, who performed the first neutron-scattering measurements on aligned single crystals of VOPO.³ These demonstrated unequivocally that the strongest exchange path in the system (J_1) was a double V-O-P-O-V link through phosphate groups in the crystallographic b direction, while the next (J_2) was a double V-O-V link between edge-sharing VO_5 square pyramids, also along \hat{b} . The V-O-V bond along \hat{a} through the apex of the pyramid, believed to be the strong ladder leg, was found to be very weak. The strength of the V-O-P-O-V bond was verified independently⁴ in the related compound $\text{VODPO}_4 \cdot \frac{1}{2}\text{D}_2\text{O}$, where it appears in isolation. These results are not unexpected, because the single electron on V^{4+} in a square pyramidal environment occupies the d_{xy} orbital in the basal (bc) plane of the unit. They lead to the interpretation of VOPO as a set of dimerized chains, with coupling ratio $\lambda = J_2/J_1 \approx 0.8$.⁵

The same experiment obtained the most detailed measurements to date for a second mode with gap 5.7 MeV. This was identified from a previous study⁶ as a candidate two-magnon bound state. In addition, the interchain coupling was deduced to be weakly ferromagnetic (FM), a result unexpected for a conventional, long superexchange path. We begin from the observation^{6,7} that frustration can act to promote bound states between excitations, and the hypothesis that the FM interchain coupling in fact results from a competition between

two AF couplings. We will deduce and justify the nature of such a frustrated, two-dimensional ($2d$) model for VOPO, and show that it provides the basis for a complete account of the magnetic properties of this material.

The structure of VOPO was determined in detail by Nguyen, Hoffman, and Sleight.⁸ The b -axis alternating chains are coupled along \hat{a} by either the V-O-V path through apical O, or by V-O-P-O-P-O-V pathways through two PO_4 groups, while c -axis coupling (see also Ref. 1) proceeds through a single phosphate unit. Quantitative superexchange calculations, particularly for extended pathways, remain beyond the scope of current understanding and computer power,⁴ particularly for the V ion. We adopt here a qualitative approach of identifying paths coupling strongly to the V d_{xy} orbital, and using consistency with experiment to construct the minimal set of necessary interactions.

We discard the possibility that the V-O-V bond along \hat{a} is significant, because its direction is orthogonal to the d_{xy} orbital. We argue instead in favor of the V-O-P-O-P-O-V path, due to the demonstrated importance of phosphate groups, and because bond angles throughout its length can remain close to 180° . Such paths connecting V ions separated only along \hat{a} (J_a), and those separated both along \hat{a} and by one ionic spacing along the chains (J_b), are in principle rather similar, which presents the possibility of frustration. However, there are two types of V-O-P-O-P-O-V path, those connecting into the phosphate groups mediating J_1 and those connecting to the O atom concerned in J_2 . If the latter were significant, one could expect in addition a strong c -axis coupling, which is not observed.³ We assume therefore that pathways of the second type are strongly suppressed by the angles and orbital configurations in the V-O-P overlap, and concentrate on the resulting $2d$ model in Fig. 1.

Here $J_1 = J$ is set to 1, λ is defined above, and $\mu_a = J_a/J$ and $\mu_b = J_b/J$ parameterize the competing V-O-P-O-P-O-V superexchange interactions. We exclude a second-neighbor intrachain coupling, due to both the lack of a suitable exchange pathway and the minimacy criterion, as it is found not to be important to any of the quantities we will compute. That $\mu_{a,b}$ may be significant is shown by a high-temperature expansion⁹ of the static susceptibility $\chi(T)$.

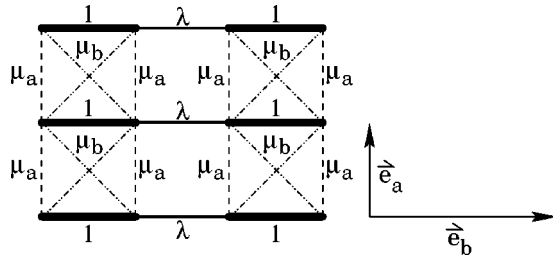


FIG. 1. Schematic representation of the VOPO system, showing frustrated coupling between dimerized chains.

This gives the Curie temperature θ_C as the sum of the interactions of a structural unit according to $\theta_C = -\frac{1}{4}J[1 + \lambda + 2\mu_a + 2\mu_b]$. Comparison with the measured $\theta_C = -84$ K (Ref. 1) suggests that the chain couplings³ alone satisfy at most 75% of the sum.

We analyze this model using the method of Ref. 9. Taking the strongest (J_1) bonds as the sites of dimers, whose singlet ground states may be excited to triplets, the interactions permit delocalization, or hopping, of the triplets. The hopping gives a kinetic energy which lowers the bond singlet-triplet gap to the physical one, and a description of a dispersive, triply-degenerate one-magnon excitation in 2D reciprocal space. While this technique is best suited to strongly dimerized systems, perturbation-theoretic calculations⁹ show rapid suppression of higher-order contributions even for rather weak dimerization, and thus internal consistency.

We have calculated the coefficients for hopping of a triplet excitation by perturbative expansion to fifth order in the parameters of Fig. 1. Contributions beyond third order indeed remain small ($\sim 3\%$), and we illustrate the method to this order. Let t_{ij} be the coefficient for the excited triplet to hop by i dimer bonds along the chain, and across j chains, and μ_{\pm} denote $\mu_a \pm \mu_b$, then

$$t_{00} = 1 - \lambda^2/16 + 3\lambda^3/64 + 3\mu_-^2/4 + 3\mu_-^2\mu_+/8, \quad (1)$$

$$t_{10} = -\lambda/4 - \lambda^2/8 + \lambda^3/64 + \lambda\mu_-^2/16,$$

$$t_{01} = \mu_-/2 - \mu_-^3/8 - 5\lambda^2\mu_-/32,$$

$$t_{20} = -\lambda^2/16 - \lambda^3/64, \quad t_{30} = -\lambda^3/128,$$

$$t_{02} = -\mu_-^2/8 - \mu_-^2\mu_+/8, \quad t_{03} = \mu_-^3/16,$$

$$t_{11} = \lambda\mu_-^2/8 - \lambda^2\mu_-/32 + \lambda\mu_- \mu_+/16,$$

$$t_{21} = 3\lambda^2\mu_-/64, \quad t_{12} = -3\lambda\mu_-^2/32.$$

The mode dispersion is given most straightforwardly by

$$\omega(\mathbf{q}) = J \sum_{ij} 2^{(2-\delta_{i0}-\delta_{j0})} t_{ij} \cos(iq_y) \cos(jq_x), \quad (2)$$

although in fact to this order one obtains a better fit by expanding the (smoother) quantity $\omega^2(\mathbf{q})$.

The measured dispersion data for the lowest-lying mode in Ref. 3, combined with the condition on θ_C , allow one to fit the optimal model parameters as the set $(J, \lambda, \mu_a, \mu_b) = (10.7 \text{ MeV}, 0.793, 0.203, 0.255)$, which correspond to the superexchange interactions

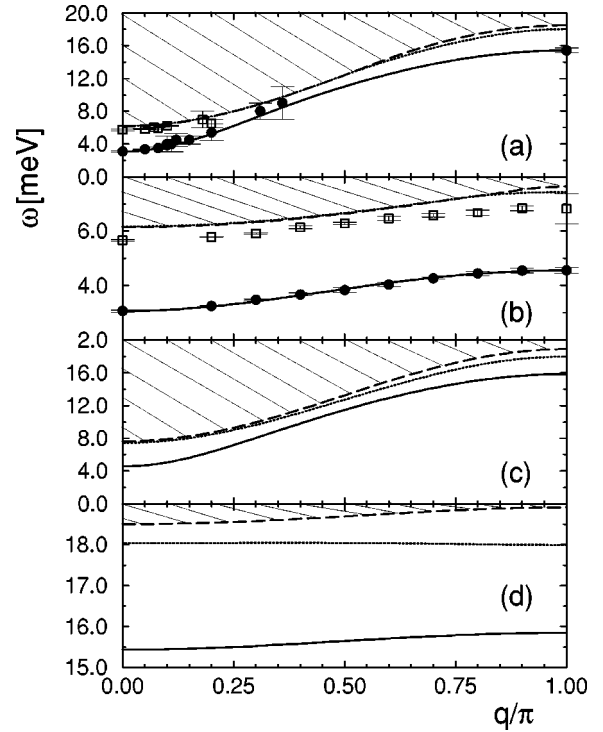


FIG. 2. Magnon dispersion (solid lines), continuum edge (dashed lines), and bound $S=1$ states (dotted lines) for (a) $(0, 2\pi - q)$, (b) $(q, 2\pi)$, (c) $(\pi, 2\pi - q)$, and (d) $(2\pi - q, \pi)$. Symbols are data taken from Ref. 3.

$$(J_1, J_2, J_a, J_b) = (10.7, 8.49, 2.17, 2.73) \text{ MeV}. \quad (3)$$

The various fits offer minor differences in the exact shape of the dispersion curve, with the higher-order calculations returning a very good description of the overall form. For clarity we show only the fifth-order fits in Figs. 2(a) and 2(b) for the reciprocal-space cuts where data is available. The results (3) may be used to predict the form of the one-magnon dispersion where it has not yet been measured, and this is shown in Figs. 2(c) and 2(d). We expect the upper band edge to be observed at 15.9 meV.

The primary features of the optimal parameter set are as follows. The alternating chains have the rather weak dimerization $\lambda \approx 0.8$, or $\delta = (1 - \lambda)/(1 + \lambda) \approx 0.11$. The interchain couplings are significant, with a magnitude 20–25% of the primary chain energy scale. The cross coupling J_b is slightly larger than the pure a -axis coupling J_a , which is required for a net FM interchain dispersion, and fully plausible from above. Figure 3 shows the density of states determined from the dispersion. The dominant feature is the logarithmic singularity at the saddle point $(\pi, 0)$, with energy 4.55 MeV. This energy, and not simply the minimum gap $\Delta = 3.1$ MeV at $(0, 0)$, will play a significant role in determining thermodynamic quantities.

We next consider two further magnetic properties for which independent measurements are available, to determine the consistency of the model and parameters. The static, uniform susceptibility $\chi(T)$ was first measured for powder samples,¹ and more recently for single crystals.¹⁰ The susceptibility to applied field H measures available excitations with $\Delta S = 1$, so is primarily a probe of the one-magnon branch. It is given in general by $\chi = -\partial^2 F / \partial H^2$, where F

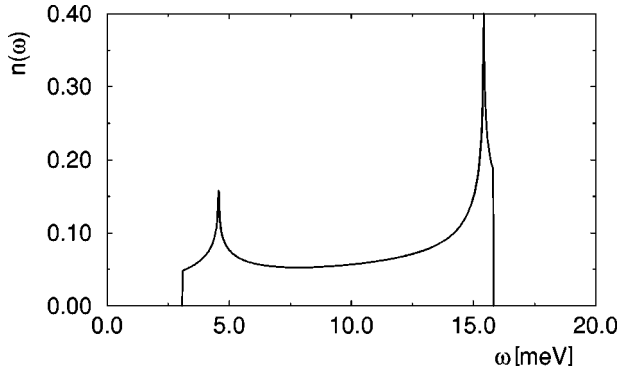


FIG. 3. Density of states for computed magnon dispersion.

$= -\beta^{-1} \ln Z$ is the free energy and $\beta^{-1} = k_B T$. In the dimer model, an excited triplet is effectively a hard-core boson, because only one such state is physically possible on each bond. Thus thermodynamic calculations require a correction from Bose statistics to exclusion statistics appropriate for triply degenerate excitations. The free energy per dimer is¹¹

$$f = -\beta^{-1} \ln \{ 1 + [1 + 2 \cosh(\beta h)] z(\beta) \}, \quad (4)$$

where h denotes $g \mu_B H$ and $z(\beta)$ is the partition function for a single mode. The susceptibility per site is then

$$\chi_0 = \beta z(\beta) / [1 + 3z(\beta)], \quad (5)$$

in which the denominator suppresses the Bose result at high T by excluding multiple mode occupation.

While the statistical factor corrects for state availability, it does not take account of magnon interaction effects. These we may include within the following mean-field scheme. Approximating any interaction term with a spin on a neighboring dimer by $J_{i,i+\delta} \mathbf{S}_i \cdot \mathbf{S}_{i+\delta} \rightarrow J_\delta \langle S_i^z \rangle S_{i+\delta}^z \equiv J_\delta m S_\delta^z$, the instantaneous magnetization per site m contributes to an effective internal magnetic field

$$h_{\text{int}} = -mJ\lambda - 2mJ(\mu_a + \mu_b) \equiv -mC. \quad (6)$$

The susceptibility is defined by $m = \chi h_{\text{ext}}$, while the magnetization $m = \chi_0 h_{\text{tot}}$, where $h_{\text{tot}} = h_{\text{ext}} + h_{\text{int}}$ is the total field at each site. Simple rearrangement yields

$$\chi = \chi_0 / (1 + C\chi_0), \quad C = J(\lambda + 2\mu_+), \quad (7)$$

as the mean-field, interaction-corrected susceptibility.

In Fig. 4(a) is shown the quantity $\chi(T)$ [Eq. (7)]. The agreement with both powder and single-crystal data is good. Qualitatively, both the exclusion statistics factor and [Fig. 4(b)] the mean-field correction are required to deduce $\chi(T)$ within this framework. Quantitatively, the temperature T_{max} of the peak in the model is 58 K, rather lower than both data sets, while χ_{max} is fractionally smaller. This latter result corroborates the presence of frustrating interactions, whose mean-field correction gives a suppression. From Fig. 4(b), the model θ_C is in excellent accord with the data.

The discrepancies between calculation and experiment may be analyzed by applying the triplet hopping theory with mean-field correction to the dimerized chain. For a chain with $\lambda = 0.8$, the resulting $\chi(T)$ is directly comparable with essentially exact numerical simulations.^{12,2} This comparison (with Figs. 2 of Refs. 12 and 2) reveals that $T_{\text{max}}^m / T_{\text{max}}^n$

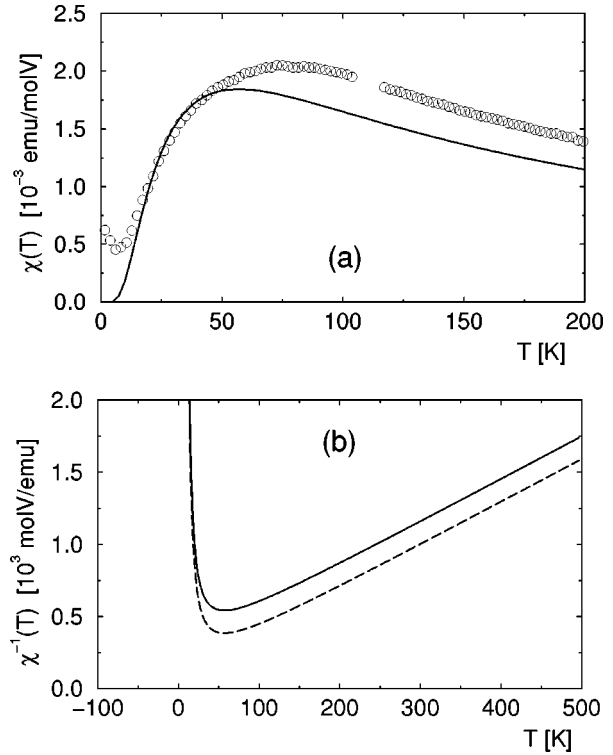


FIG. 4. (a) $\chi(T)$ from model parameter set. Deviations from measured data (Ref. 10) are discussed in text. (b) $\chi^{-1}(T)$ with (solid line) and without (dashed) mean-field correction.

≈ 0.75 , while $\chi_{\text{max}}^m / \chi_{\text{max}}^n \approx 1.2$, where superscripts m and n denote model and numerical results, respectively. The first ratio is very similar to the discrepancy between model and experiment above. The second suggests further that in $1d$ the mean-field correction is not sufficient to reproduce interaction-induced suppression of χ , whereas improved agreement is achieved in $2d$. We conclude that deviations from the data arise primarily because the calculational scheme cannot fully account for magnon interactions, and not due to any intrinsic shortcomings of the model.

Electron-spin resonance (ESR) experiments have also been performed on powder and crystalline VOPO samples, and we focus on the latter.¹⁰ For linearly polarized (microwave) radiation, which excites transitions of $\Delta S^z = \pm 1$, the power absorption is given¹³ by the imaginary part of the susceptibility

$$\chi''(\omega) = \pi \delta(\hbar\omega - h) \sinh(\beta\hbar\omega) \int \frac{d^2k}{(2\pi)^2} e^{-\beta\omega(\mathbf{k})}. \quad (8)$$

Including the hard-core boson constraint as above, the intensity at the resonance frequency $\hbar\omega = h$ is

$$I(\beta) \propto \frac{\sinh(\beta h) z(\beta)}{1 + [1 + 2 \cosh(\beta h)] z(\beta)}. \quad (9)$$

This quantity contains in principle the mean-field correction in the form $h = h_{\text{ext}} - Cm$. However, for the strongest resonance at 134 GHz ~ 7 K, the \sinh function is linear at temperatures on the order of Δ , and alterations of h affect only the prefactor.

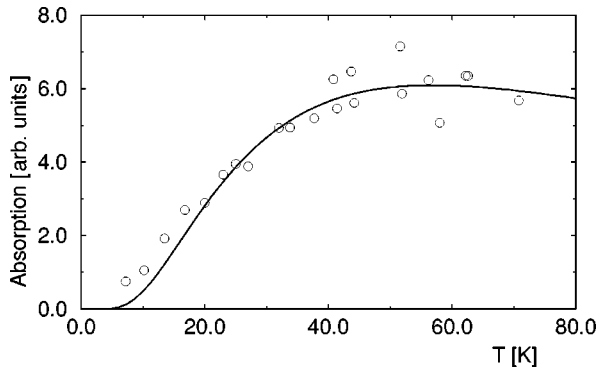


FIG. 5. ESR absorption from model parameter set, showing excellent consistency with observation (Ref. 10).

The calculated ESR absorption at 134 GHz is shown in Fig. 5 with the data of Ref. 10. The excellent agreement indicates the importance of the 2D density of states, in particular the energy of the logarithmic singularity (Fig. 3). While the ESR absorption is often considered to measure a $q=0$ property akin to $\chi(T)$, we note here a significant difference between the two in experiment. Theoretically, the triplet hopping approach yields a single energy scale for both quantities, which is in more satisfactory agreement with the ESR absorption, indicating that this is rather less sensitive than $\chi(T)$ to magnon interactions.

We conclude with a brief analysis of possible bound states of two magnons with the computed dispersion, to seek an explanation for the observed second mode. The initial perturbative problem, represented generally as $H=H_0 + \alpha H'$, may be brought by a continuous, unitary transformation¹⁴ to a new Hamiltonian H_{eff} which conserves triplet number ($[H_{\text{eff}}, H_0]=0$). This procedure is conducted perturbatively in α to generate a series for H_{eff} . The action of H_{eff} on the sector with one triplet gives the one-magnon dispersion, while on the two-triplet sector with total spin $S=1$ it yields the two-magnon continuum and contains in addition magnon interactions. At fixed momentum one obtains a two-body problem soluble by Lanczos tridiagonalization, in particular for the energy of (triplet) bound states. The number of interaction coefficients rises very rapidly with or-

der n in α . We have completed calculations for $n=3$ and 4, finding only small alterations ($\approx 2\%$ of the continuum edge energy), but caution that these remain potentially significant.

The predicted dispersion curves for the two-magnon bound state, computed at fourth order, are shown as the dotted lines in Fig. 2. We find that with the parameters fixed as above, the bound state does appear as an excitation mode below the continuum over a large part of the Brillouin zone. However, this is not the case close to the band minimum, where it is lost in the continuum. While we thus do not always find a second mode below 2Δ in a consistent treatment, the discrepancy between the computed bound state and the observed resonance is not large: it is reasonable to postulate that forthcoming refinement of this calculation, and possible extension of the model to include further interactions, will indeed yield a quantitative explanation of the second mode.

In summary, we have presented a model for frustrated, 2D coupling in $(\text{VO})_2\text{P}_2\text{O}_7$. The model gives an excellent and fully consistent account of the available data concerning elementary excitations, namely the one-magnon dispersion, static susceptibility, and ESR absorption. We use it to predict the dispersion in the entire Brillouin zone, and to indicate the origin of the observed, low-lying second excitation mode as a triplet two-magnon bound state.

During completion of this work, we became aware of the contribution of Weisse, Bouzerar, and Fehske¹⁵. These authors investigated the same model, albeit without the physical justification presented here, by diagonalization on small (up to 4×8) clusters. Their results are qualitatively in good agreement with our expectation that frustration should promote bound states. Quantitatively, the parameters chosen differ considerably, and we would not expect to see good agreement with susceptibility and ESR data.

We are grateful to U. Löw, B. Lüthi, S. Nagler, H. Schwenk, and particularly D. A. Tennant for invaluable discussions and provision of data. We thank also E. Müller-Hartmann for helpful conversations, and C. Knetter for assistance with the calculation of H_{eff} . G.S.U. was supported by an individual grant and by SFB 341 of the DFG. B.N. wishes to acknowledge the generosity of the Treubelfonds.

¹D. C. Johnston, J. W. Johnson, D. P. Goshorn, and A. J. Jacobson, Phys. Rev. B **35**, 219 (1987).

²T. Barnes and J. Riera, Phys. Rev. B **50**, 6817 (1994).

³A. W. Garrett, S. E. Nagler, D. A. Tennant, B. C. Sales, and T. Barnes, Phys. Rev. Lett. **79**, 745 (1997).

⁴D. A. Tennant, S. E. Nagler, A. W. Garrett, T. Barnes, and C. C. Torardi, Phys. Rev. Lett. **78**, 4998 (1997).

⁵T. Barnes, J. Riera, and D. A. Tennant, cond-mat/9801224, Phys. Rev. B (to be published).

⁶G. S. Uhrig and H. J. Schulz, Phys. Rev. B **54**, R9624 (1996); Phys. Rev. B **58**, 2900 (1998).

⁷G. Bouzerar, A. P. Kampf, and G. Japaridze, Phys. Rev. B **58**, 3117 (1998).

⁸P. T. Nguyen, R. D. Hoffman, and A. W. Sleight, Mater. Res. Bull. **30**, 1055 (1995).

⁹G. S. Uhrig, Phys. Rev. Lett. **79**, 163 (1997).

¹⁰A. V. Prokofiev, F. Büllensfeld, W. Assmus, H. Schwenk, D. Wichert, U. Löw, and B. Lüthi, Eur. Phys. J. B **5**, 313 (1998).

¹¹M. Troyer, H. Tsunetsugu, and D. Würtz, Phys. Rev. B **50**, 13 515 (1994).

¹²J. C. Bonner, H. W. J. Blöte, J. W. Bray, and I. S. Jacobs, J. Appl. Phys. **50**, 1810 (1979).

¹³I. Affleck, Phys. Rev. B **46**, 9002 (1992).

¹⁴F. J. Wegner, Ann. Phys. (Leipzig) **3**, 77 (1994).

¹⁵A. Weisse, G. Bouzerar, and H. Fehske, cond-mat/9805374 (unpublished).